This article was downloaded by: [University of California, San Diego]
On: 07 August 2012, At: 12:25
Publisher: Taylor & Francis
Informa Ltd Registered in England and Wales Registered Number: 1072954 Registered office: Mortimer House, 37-41 Mortimer Street, London W1T 3JH, UK

Molecular Crystals and Liquid Crystals
Publication details, including instructions for authors and subscription information:
http://www.tandfonline.com/loi/gmcl20

# Characterization of Langmuir Films of Naphthalimide Dyes Mixed with 4-Heptyl-4′-Cyanobiphenyl (7CB)

N. Bielejewska [a], R. Stolarski [b] & D. Bauman [a]

[a] Faculty of Technical Physics, Poznań University of Technology, Poznań, Poland

[b] Institute of Polymer Technology and Dyes, Łódź University of Technology, Łódź, Poland

Version of record first published: 14 Jun 2011

To cite this article: N. Bielejewska, R. Stolarski & D. Bauman (2011): Characterization of Langmuir Films of Naphthalimide Dyes Mixed with 4-Heptyl-4′-Cyanobiphenyl (7CB), Molecular Crystals and Liquid Crystals, 544:1, 136/[1124]-149/[1137]

To link to this article: http://dx.doi.org/10.1080/15421406.2011.569287

PLEASE SCROLL DOWN FOR ARTICLE

Full terms and conditions of use: http://www.tandfonline.com/page/terms-and-conditions

This article may be used for research, teaching, and private study purposes. Any substantial or systematic reproduction, redistribution, reselling, loan, sub-licensing, systematic supply, or distribution in any form to anyone is expressly forbidden.

The publisher does not give any warranty express or implied or make any representation that the contents will be complete or accurate or up to date. The accuracy of any instructions, formulae, and drug doses should be independently verified with primary sources. The publisher shall not be liable for any loss, actions, claims, proceedings, demand, or costs or damages whatsoever or howsoever caused arising directly or indirectly in connection with or arising out of the use of this material.

*Mol. Cryst. Liq. Cryst.*, Vol. 544: pp. 136/[1124]–149/[1137], 2011
Copyright © Taylor & Francis Group, LLC
ISSN: 1542-1406 print/1563-5287 online
DOI: 10.1080/15421406.2011.569287

Taylor & Francis
Taylor & Francis Group

# Characterization of Langmuir Films of Naphthalimide Dyes Mixed with 4-Heptyl-4′-Cyanobiphenyl (7CB)

N. BIELEJEWSKA,[1] R. STOLARSKI,[2] AND D. BAUMAN[1]

[1]Faculty of Technical Physics, Poznań University of Technology, Poznań, Poland
[2]Institute of Polymer Technology and Dyes, Łódź University of Technology, Łódź, Poland

Downloaded by [University of California, San Diego] at 12:25 07 August 2012

*Langmuir films formed of derivatives of 4-aminonaphthalimide and their binary mixtures with the liquid crystal 4-heptyl-4′-cyanobiphenyl (7CB) have been studied. The films have been characterized by the surface pressure–area (π-A) and surface potential–area (ΔV-A) isotherms and by Brewster angle microscopy (BAM). Additionally, the electronic absorption spectra of a monolayer on the water surface at different stages of the film formation were recorded. On the basis of these spectra the conclusions about the ability of the dye molecules to form self-aggregates at the air–water interface have been drawn.*

**Keywords** BAM image; electronic absorption; Langmuir film; liquid crystal; naphthalimide dye; surface potential

## 1. Introduction

The previous study have shown that some of 1,8-naphthalimide dyes are characterized by brilliant yellow color and emit light with high quantum fluorescence yield in the spectral region advantageous for human eye. Moreover, these dyes are stable for sun light, orient well in liquid crystals and do not destabilize the mesophase region of the host [1,2]. Therefore, they are very attractive for the potential application in passive and active guest-host liquid crystal displays [3]. Recently, due to efficient luminescence of 1,8-naphthalimide dyes, the possibility of their utilization as an active layer in organic light emitting diodes (OLEDs) has been tested [4–7]. Organic material used in the active layer in OLEDs need to be characterized by a good charge transport which usually increases with increasing order of molecules. One of the possibilities to achieve highly ordered molecular layers is utilization of Langmuir-Blodgett (LB) technique [8]. As it was found, most of 1,8-naphthalimide dyes can

Address correspondence to N. Bielejewska, Faculty of Technical Physics, Poznań University of Technology, 60-965 Poznań, Poland. E-mail: natalia.bielejewska@doctorate.put.poznan.pl

create stable LB films themselves, while others need to be stabilized, *e.g.*, by fatty acids or thermotropic liquid crystals [4–7].

One of the prerequisites to achieve LB film is fabrication of a compressible and stable Langmuir layer. Investigation of such layers formed by some novel 1,8-naphthalimide dyes (derivatives of 4-aminonaphthalimide) is the subject of this work. We present here the results of the study of Langmuir films formed of twelve naphthalimide dyes and their mixtures with 4-heptyl-4′-cyanobiphenyl (7CB) used as stabilizing matrix. The aim of the investigations was to determine the molecular organization and mutual interactions among dye and liquid crystal molecules in monolayers formed at air–water interface.

Downloaded by [University of California, San Diego] at 12:25 07 August 2012

## 2. Experimental Methods

The set of the dyes investigated consists of twelve derivatives of 4-aminonaphthalimide. Their synthesis is described in [9]. The chemical structure of the dyes,

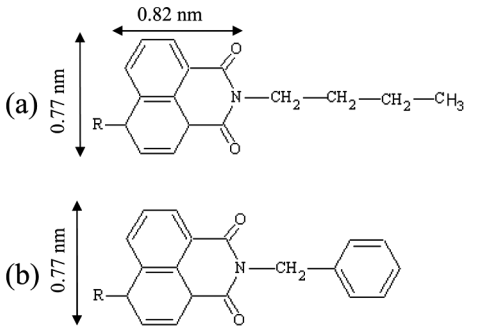


| Dye code | | R |
|---|---|---|
| (a) | (b) | |
| **1** | **7** | 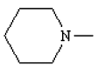 |
| **2** | **8** | 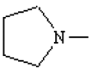 |
| **3** | **9** | $CH_3(CH_2)_3NH$ — |
| **4** | **10** | $(CH_2)_3N$ — |
| **5** | **11** | 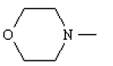 |
| **6** | **12** | 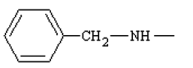 |

**Figure 1.** Molecular structure of dyes investigated.

confirmed by $^1$H NMR analysis, is given in Figure 1. The liquid crystal 4-*n*-heptyl-4′-cyanobiphenyl, 7CB was purchased from the Dąbrowski Laboratory at the Military University of Technology, Warsaw (Poland) and was used without further purification. Solutions of dyes and 7CB were prepared in chloroform. Chloroform was spectroscopic quality (Uvasol, 99.9%) obtained from Merck.

The surface pressure ($\pi$) and surface potential ($\Delta$V) *versus* the mean molecular area isotherm diagrams for Langmuir films were recorded by use of a Minitrough 2 (KSV Instruments Ltd., Finland). Water deionized by a Millipore Milli-Q system (Millipore Corporation, Austria) with a resistivity of 18.2 M$\Omega \cdot$cm was used as a subphase. The temperature of the subphase was maintained by a cooling circulator and kept constant at $(20 \pm 1)^\circ$C. The surface pressure was monitored by a Wilhelmy plate balance with an accuracy of $\pm 0.1$ mN/m, and the surface potential was measured using the vibrating plate method by means of a SPOT 1 head from KSV with an accuracy of $\pm 10$ mV. Further experimental details about Langmuir films preparation are given elsewhere [5,6]. All measurements were repeated on fresh subphases three to five times to confirm reproducibility.

The morphology of the Langmuir films was visualized by means of a Brewster angle microscope (BAM). The instrument we used is based on Hoenig and Moebius setup [10] and was built in our laboratory. The image features were observed with a lateral resolution of $\approx 5\,\mu$m.

Absorption spectra of Langmuir films were recorded in UV-Vis region by use of a spectrophotometer Varian CARY 400. For the absorption measurements of a spread monolayer *in situ*, the spectrophotometer was equipped with optical fibers and a photodiode array detector supplied by Varian. Further details of this setup are given in Ref. [7].

## 3. Results and Discussion

### *3.1. Surface Pressure and Surface Potential Versus Mean Molecular Area Isotherms*

The surface pressure–mean molecular area ($\pi$-A) isotherms for Langmuir films of derivatives of 4-aminonaphthalimide under investigation had been already presented in Ref. [6]. They revealed that ten of twelve dyes are able to form stable and compressible floating monolayer at the air–water interface, although the shape of isotherms is different for various dyes. It depends strongly on the molecular structure of the groups substituted to the main core of the dyes molecules. Simultaneously to surface pressure–mean molecular area isotherms the surface potential–mean molecular area isotherms were recorded. The dependence of the surface potential on the area available for one molecule provides information about the polar molecules organization during the Langmuir film formation process, especially in the early stages of the film creation, before the change of the surface pressure occurs. Figure 2 shows $\Delta$V-A (solid curve) and $\pi$-A (dashed curve) isotherms for 7CB (a) and dye **8**/7CB mixtures at various molar fraction ($X_M$) of the dye (b-e) and pure dye 8(f), as examples. Table 1 contains the characteristic value of $\pi$-A and $\Delta$V-A isotherms for Langmuir films of dyes **1**–**12** and their binary mixtures with 7CB at different $X_M$. $A_0^\pi$ and $A_0^{\Delta V}$ are the values of the areas at which the surface pressure and surface potential, respectively, begin to rise, $A_C$, $\pi_C$ and $\Delta V_C$ are the values of, respectively, the area, the surface pressure, and the surface potential at the collapse

Downloaded by [University of California, San Diego] at 12:25 07 August 2012

Downloaded by [University of California, San Diego] at 12:25 07 August 2012

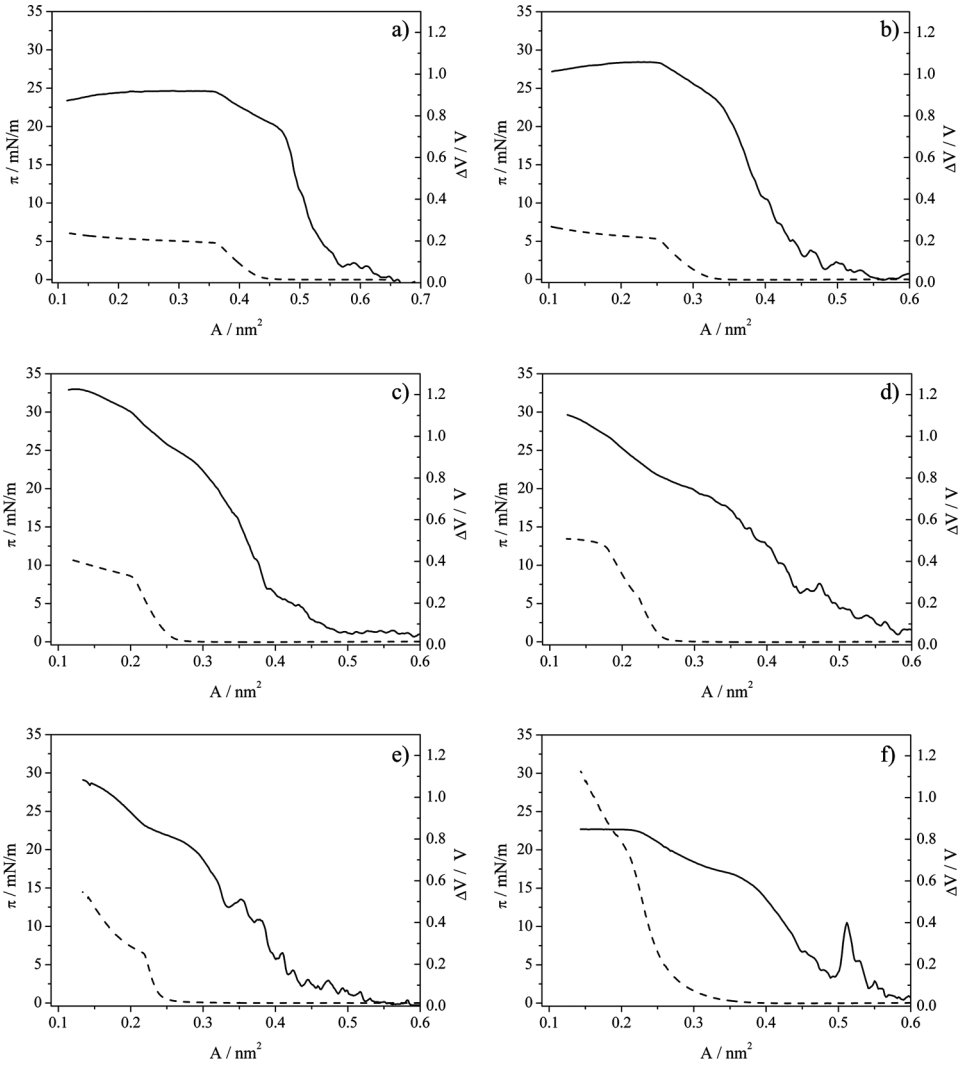


**Figure 2.** Surface potential ΔV (solid curve) and surface pressure $\pi$ (dashed curve) as a function of the mean molecular area, $A$ for Langmuir films of 7CB (a), and **8**/7CB mixtures at $X_M$ equal to 0.2 (b), 0.4 (c), 0.6 (d), 0.8 (e) and pure dye **8** (f).

point. The collapse point is recognized as the point in the $\pi$-A isotherm where the ratio $\partial\pi/\partial A$ starts to decrease.

More information about the Langmuir films formed of derivatives of 4-aminonaphthalimide and their mixtures with 7CB can give the compressibility coefficient, defined as [11]:

$$C = -\frac{1}{A_1}\frac{A_2 - A_1}{\pi_2 - \pi_1}, \tag{1}$$

where $A_1$ and $A_2$ correspond to the area per molecule at the surface pressures $\pi_1$ and $\pi_2$. The values of $\pi$ were taken at the beginning and the end of the linear region of

**Table 1.** Features of $\pi$-A and $\Delta$V-A isotherms for Langmuir films of dyes **1**–**12** mixed with 7CB on the water surface

| Compound | $A_0^{\pi}/nm^2$ | $A_C/nm^2$ | $\pi_C/mN \cdot m^{-1}$ | C/m/N | $A_0^{\Delta V}/nm^2$ | $\Delta V_C/V$ |
|---|---|---|---|---|---|---|
| 7CB | 0.47 | 0.37 | 4.9 | 34.9 | 0.65 | 0.91 |
| **1**/7CB | | | | | | |
| $X_M = 0.2$ | 0.47 | 0.32 | 6.0 | 44.2 | 0.66 | 0.37 |
| $X_M = 0.4$ | 0.41 | 0.26 | 8.7 | 33.4 | 0.74 | 0.50 |
| $X_M = 0.6$ | 0.41 | 0.25 | 9.4 | 30.0 | 0.67 | 0.54 |
| $X_M = 0.8$ | 0.43 | 0.30 | 9.0 | 26.6 | 0.70 | 0.45 |
| $X_M = 1.0$ | 0.52 | 0.36 | 8.7 | 28.0 | –[a] | –[a] |
| **2**/7CB | | | | | | |
| $X_M = 0.2$ | 0.46 | 0.31 | 5.6 | 43.2 | 0.54 | 0.81 |
| $X_M = 0.4$ | 0.37 | 0.25 | 8.3 | 34.5 | 0.58 | 0.78 |
| $X_M = 0.6$ | 0.37 | 0.25 | 10.0 | 28.2 | 0.62 | 0.68 |
| $X_M = 0.8$ | 0.38 | 0.24 | 9.8 | 29.6 | 0.67 | 0.61 |
| $X_M = 1.0$ | 0.38 | 0.28 | 9.8 | 18.4 | –[a] | –[a] |
| **3**/7CB | | | | | | |
| $X_M = 0.2$ | 0.50 | 0.35 | 7.1 | 29.9 | 0.64 | 0.94 |
| $X_M = 0.4$ | 0.44 | 0.27 | 9.8 | 26.9 | 0.70 | 0.77 |
| $X_M = 0.6$ | 0.43 | 0.25 | 14.2 | 22.7 | –[a] | –[a] |
| $X_M = 0.8$ | 0.42 | 0.23 | 15.7 | 21.6 | –[a] | –[a] |
| $X_M = 1.0$ | 0.40 | 0.23 | 16.2 | 20.4 | –[a] | –[a] |
| **4**/7CB | | | | | | |
| $X_M = 0.2$ | 0.38 | 0.28 | 5.8 | 36.0 | 0.56 | 0.46 |
| $X_M = 0.4$ | 0.32 | 0.21 | 7.8 | 31.4 | 0.70 | 0.89 |
| $X_M = 0.6$ | 0.25 | 0.14 | 10.1 | 29.8 | 0.72 | 0.93 |
| $X_M = 0.8$ | 0.28 | 0.16 | 10.4 | 30.4 | 0.55 | 0.82 |
| $X_M = 1.0$ | 0.36 | 0.25 | 10.9 | 17.9 | –[a] | –[a] |
| **5**/7CB | | | | | | |
| $X_M = 0.2$ | 0.37 | 0.26 | 5.9 | 33.4 | 0.68 | 0.50 |
| $X_M = 0.4$ | 0.32 | 0.21 | 7.2 | 31.0 | 0.63 | 0.73 |
| **6**/7CB | | | | | | |
| $X_M = 0.2$ | 0.39 | 0.30 | 6.8 | 28.2 | 0.70 | 0.56 |
| $X_M = 0.4$ | 0.37 | 0.24 | 13.2 | 21.5 | 0.72 | 0.55 |
| $X_M = 0.6$ | 0.36 | 0.25 | 11.6 | 20.5 | 0.65 | 0.32 |
| $X_M = 0.8$ | 0.40 | 0.30 | 9.1 | 19.5 | 0.70 | 0.28 |
| $X_M = 1.0$ | 0.38 | 0.29 | 8.0 | 22.1 | –[a] | –[a] |
| **7**/7CB | | | | | | |
| $X_M = 0.2$ | 0.38 | 0.27 | 5.3 | 45.4 | 0.70 | 0.32 |
| $X_M = 0.4$ | 0.35 | 0.24 | 7.6 | 33.4 | 0.69 | 0.29 |
| $X_M = 0.6$ | 0.38 | 0.27 | 6.0 | 35.4 | 0.60 | 0.20 |
| $X_M = 0.8$ | 0.40 | 0.31 | 3.8 | 32.5 | 0.65 | 0.28 |
| $X_M = 1.0$ | 0.42 | 0.36 | 2.6 | 28.8 | –[a] | –[a] |
| **8**/7CB | | | | | | |
| $X_M = 0.2$ | 0.35 | 0.25 | 5.3 | 40.9 | 0.53 | 1.05 |
| $X_M = 0.4$ | 0.28 | 0.20 | 8.4 | 24.0 | 0.50 | 0.97 |

(*Continued*)

Downloaded by [University of California, San Diego] at 12:25 07 August 2012

**Table 1.** Continued

| Compound | $A_0^{\pi}/nm^2$ | $A_C/nm^2$ | $\pi_C/mN \cdot m^{-1}$ | C/m/N | $A_0^{\Delta V}/nm^2$ | $\Delta V_C/V$ |
|---|---|---|---|---|---|---|
| $X_M = 0.6$ | 0.28 | 0.18 | 12.4 | 26.0 | 0.68 | 0.86 |
| $X_M = 0.8$ | 0.27 | 0.22 | 6.4 | 14.6 | 0.58 | 0.95 |
| $X_M = 1.0$ | 0.37 | 0.21 | 19.0 | 12.0 | 0.55 | 0.85 |
| **9**/7CB | | | | | | |
| $X_M = 0.2$ | 0.37 | 0.28 | 5.7 | 38.8 | 0.65 | 0.79 |
| $X_M = 0.4$ | 0.39 | 0.25 | 12.0 | 21.5 | 0.70 | 0.68 |
| $X_M = 0.6$ | 0.35 | 0.23 | 11.9 | 20.5 | 0.71 | 0.76 |
| $X_M = 0.8$ | 0.35 | 0.27 | 11.2 | 15.7 | 0.70 | 0.49 |
| $X_M = 1.0$ | 0.41 | 0.32 | 11.0 | 12.8 | 0.73 | 0.41 |
| **10**/7CB | | | | | | |
| $X_M = 0.2$ | 0.42 | 0.28 | 6.3 | 37.8 | 0.51 | 1.43 |
| $X_M = 0.4$ | 0.32 | 0.21 | 10.4 | 24.9 | 0.42 | 1.07 |
| $X_M = 0.6$ | 0.29 | 0.17 | 13.0 | 28.0 | 0.63 | 1.07 |
| $X_M = 0.8$ | 0.29 | 0.17 | 7.9 | 40.1 | –[a] | –[a] |
| $X_M = 1.0$ | 0.28 | 0.19 | 5.6 | 32.5 | 0.53 | 1.00 |
| **11**/7CB | | | | | | |
| $X_M = 0.2$ | 0.40 | 0.29 | 4.8 | 39.7 | 0.65 | 0.58 |
| $X_M = 0.4$ | 0.36 | 0.23 | 5.8 | 38.7 | 0.70 | 0.76 |
| $X_M = 0.6$ | 0.25 | 0.16 | 6.6 | 39.3 | 0.73 | 0.72 |
| **12**/7CB | | | | | | |
| $X_M = 0.2$ | 0.37 | 0.28 | 6.7 | 28.0 | 0.65 | 0.48 |
| $X_M = 0.4$ | 0.35 | 0.25 | 10.8 | 20.6 | 0.68 | 0.52 |
| $X_M = 0.6$ | 0.37 | 0.28 | 6.8 | 23.6 | 0.66 | 0.42 |
| $X_M = 0.8$ | 0.37 | 0.32 | 5.9 | 13.8 | 0.62 | 0.45 |
| $X_M = 1.0$ | 0.50 | 0.35 | 10.8 | 12.6 | 0.68 | 0.51 |

[a]Impossible to record.

the $\pi$-A isotherm. In Table 1 the values of C for the Langmuir films of 7CB and dye/7CB mixtures are presented. It is seen that in the most cases the compressibility decreases with increasing the dye content in the mixture, which means that the addition of the dye to the liquid crystal improves the rigidity of the monolayer at the water surface.

The run of $\Delta V$-A isotherm of 7CB is very similar to that of 8CB and 8PCH [12], likewise as it is in the case of $\pi$-A isotherm [13]. The rise of $\Delta V$ is observed earlier ($A = 0.65\,nm^2$) than the onset of the increase of $\pi$ ($A = 0.47\,nm^2$). $\Delta V$ increases rapidly to the value of 711 mV, next increases a little and reaches the value of 910 mV at the collapse point at $A = 0.37\,nm^2$. Behind the collapse point both $\pi$ and $\Delta V$ remain constant. The addition of the dye to 7CB affects considerably the surface potential. Although the dye molecules are only weakly polar, they influences the organization of strongly polar 7CB molecules in the monolayer at the water surface and as a result the resultant polar ordering varies. The surface potential at the collapse point for dye **8** is smaller than that for the liquid crystal and in **8**/7CB mixtures $\Delta V_C$ decreases with increasing dye content. As it is seen from Table 1, for other dyes mixed with 7CB the regular

Downloaded by [University of California, San Diego] at 12:25 07 August 2012

behavior of $\Delta V_C$ with the change of $X_M$ is not always observed, similarly as it is for $\Delta V$ beyond the collapse point. In the case of dyes **2, 3** and **6** and their mixtures with 7CB at reducing mean molecular area $\Delta V$ remains almost constant, likewise as in the case of 7CB (Fig. 3a). For dyes **4, 5** and **11** the small but distinct increase of $\Delta V$ in this region of the area is found. Other dyes reveal the significant increase of $\Delta V$, especially at higher $X_M$, as it is observed e.g., for dye **8**/7CB mixtures (Fig. 3c-e). This indicates the different change of the molecular organization for various dye/7CB mixtures in the Langmuir films compressed beyond the collapse point.

Downloaded by [University of California, San Diego] at 12:25 07 August 2012

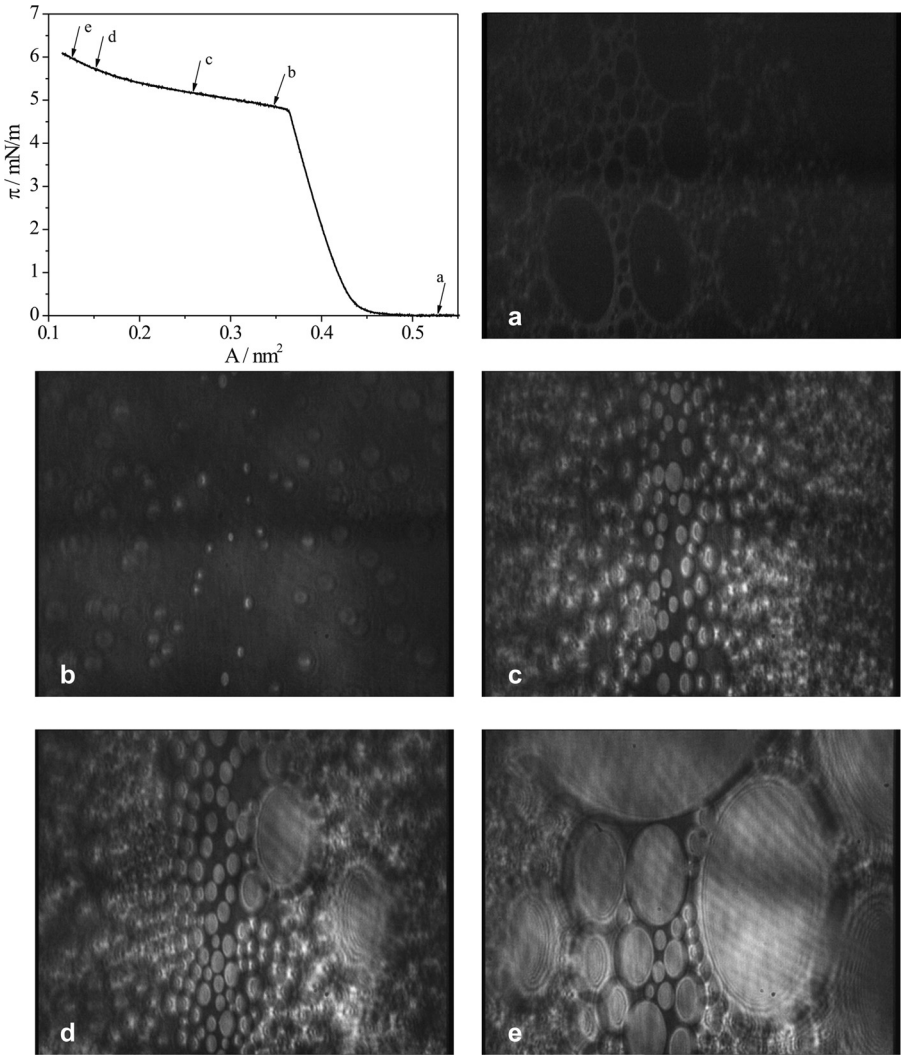


**Figure 3.** Surface pressure-mean molecular area isotherm of 7CB and BAM images obtained during the compression. The scale of the images is $0.35 \times 0.30\,nm^2$.

### *3.2 Brewster Angle Microscope Images*

Additional information about the organization of molecules at the air–water interface gives the Brewster angle microscopy (BAM), which enables the direct observation of the texture of Langmuir films. Figure 3 illustrates the change of the textures of 7CB monolayer during compression process. The marks on $\pi$-A isotherm indicate the compression stages at which BAM images were recorded. In the region of coexistence of the gas and liquid phases (Fig. 3a) we observed condensed monolayer islands in equilibrium with a foam-like structure. As the surface pressure $\pi$ was raised ($A = 0.47$–$0.37\,nm^2$), the islands packed together into a completely compressed monolayer, giving a homogeneous picture (data not shown). Just after the collapse point, when the surface pressure remains constant (the plateau region), small brighter domains were observed (Fig. 3b). With the reduction of the film area the sizes of domains grew, they deformed and joined together (Fig. 3c-e). The images obtained are very similar to those found previously for 8CB [13,14] for which the creation of the interdigitated bilayer on the top of the first monolayer being in contact with the water was postulated [14]. The representative examples of BAM images recorded for the dye/7CB mixtures are seen in Figures 4–6. In the case of dye **2** mixed with 7CB at $X_M = 0.1$, beyond the collapse point (Fig. 4a) small flat domains, resembling those of 7CB, were observed. However, at reducing the available area, the brighter objects with interference rings appeared (Fig. 4b, c).

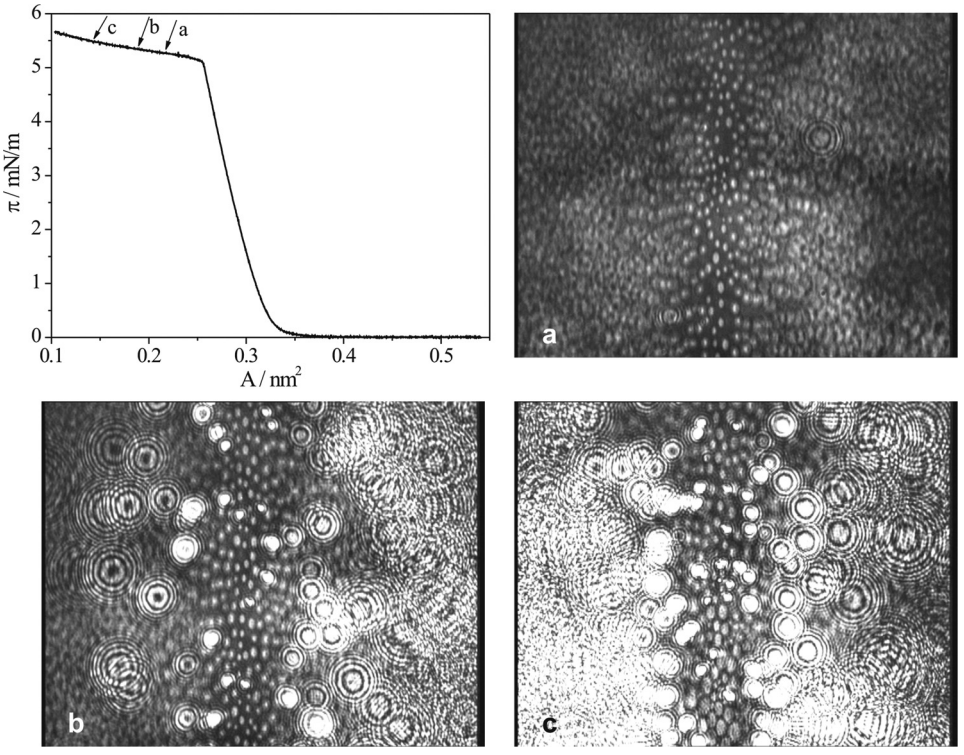


**Figure 4.** Surface pressure-mean molecular area isotherm of **2**/7CB mixture at $X_M = 0.1$ and BAM images obtained during the compression. The scale of the images is $0.35 \times 0.30\,nm^2$.

Downloaded by [University of California, San Diego] at 12:25 07 August 2012

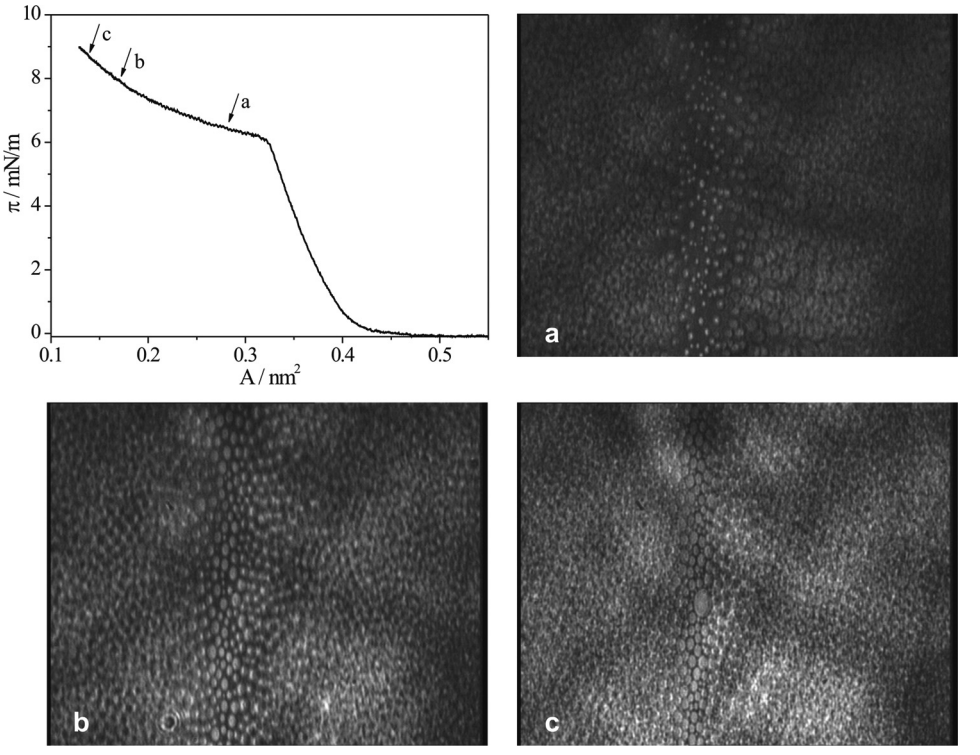


**Figure 5.** Surface pressure-mean molecular area isotherm of **10**/7CB mixture at $X_M = 0.1$ and BAM images obtained during the compression. The scale of the images is $0.35 \times 0.30\,nm^2$.

As it was suggested in Ref [13]., such images are characteristic for the creation of 3D droplet-like domains. With the increase of the dye content in the mixture the number of such objects increased, as it is seen in Figure 6a. Similar BAM images were obtained for dyes **3** and **6**. For dyes **4, 5** and **11** the 3D domains were observed not before the dye content was high enough, as shows Figure 6b for dye **4** mixed with 7CB at $X_M = 0.3$. The mixtures of other dyes with 7CB formed flat oval domains at small $X_M$, which is illustrates for dye **10**/7CB mixture in Figure 5a. With the reducing area (Fig. 5b, c) and increasing dye content (Fig. 6c) the domains increasingly close to each other, but did not join together. As for these dyes mixed with the liquid crystal the rise of the surface potential behind the collapse point was observed (see previous section), it can be suggested that during compression process the polar molecules of 7CB, stiffened by the dye molecules, assume more and more vertical alignment with respect to the water surface. This suggestion stems from the fact that, according to Helmholtz equation [15], the surface potential is directly proportional to the vertical component of the molecular dipole moment. In the case of dyes **2**–**6** and **11** mixed with 7CB, $\Delta V$ beyond the collapse remains constant or increases only slightly, which indicates that the inclination of the molecules in the monolayer being in contact with the water does not change. Instead, when the available area is too small for all the molecules to remain on the surface, they are pushed up and create 3D objects.

Downloaded by [University of California, San Diego] at 12:25 07 August 2012

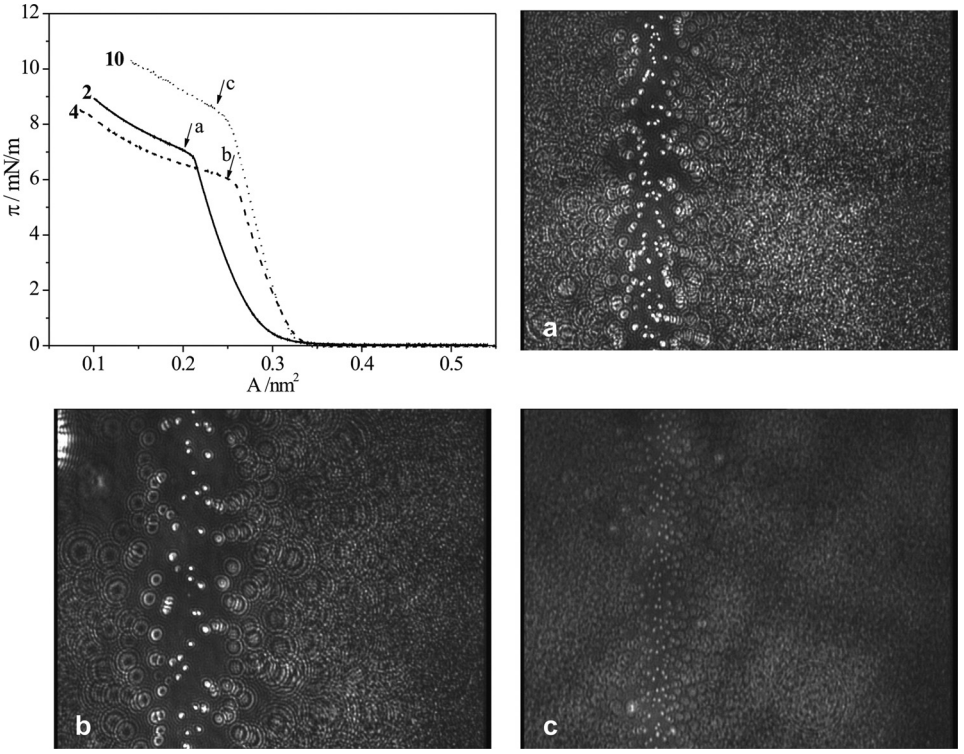


**Figure 6.** Surface pressure-mean molecular area isotherms of **2**/7CB (a), **4**/7CB (b) and **10**/7CB (c) mixtures ($X_M = 0.3$) and BAM images obtained during the compression. The scale of the images is $0.35 \times 0.30\,nm^2$.

### *3.3. Electronic Absorption Spectra of Langmuir Films*

For all twelve dyes investigated and their mixtures with 7CB for $X_M \geq 0.4$, the absorption spectra *in situ* for monolayers floating on the air–water interface were

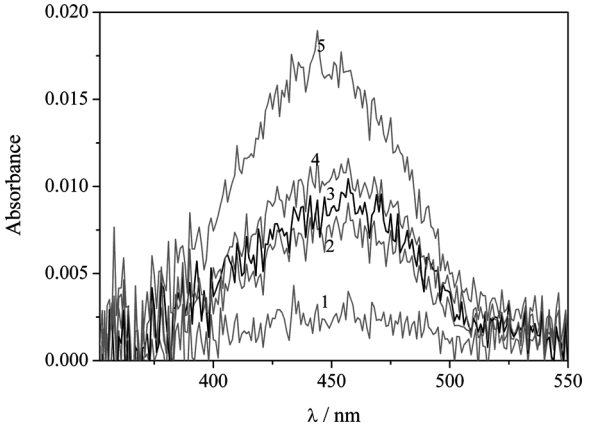


**Figure 7.** Long-wavelength absorption spectra *in situ* of the Langmuir film formed of dye **3** at $\pi = 0$ (1), $\pi = 5$ (2), $\pi = 10$ (3), $\pi = 16.2$ (4), and $\pi = 16.6$ (5) mN/m.

Downloaded by [University of California, San Diego] at 12:25 07 August 2012

**Table 2.** The position of absorption maximum ($\lambda_{max}$) and half-bandwidth of the long-wavelength absorption band ($\delta$) of **1**–**12** mixtures in Langmuir films and dyes **1**–**12** dissolved in chloroform at $X_M = 10^{-7}$

| | | Langmuir film | | chloroform | |
|---|---|---|---|---|---|
| Dye code | $X_M$ | $\lambda_{max}$/nm $\Delta\lambda = \pm 1$ nm | $\delta$/cm$^{-1}$ $\Delta\delta = \pm 50$ cm$^{-1}$ | $\lambda_{max}$/nm $\Delta\lambda = \pm 1$ nm | $\delta$/cm$^{-1}$ $\Delta\delta = \pm 10$ cm$^{-1}$ |
| **1** | 0.4 | 413 | 4700 | 410 | 4460 |
| | 0.6 | 410 | 5350 | | |
| | 0.8 | 415 | 4750 | | |
| **2** | 0.4 | 458 | 3850 | 442 | 3470 |
| | 0.6 | 460 | 4100 | | |
| | 0.8 | 457 | 4050 | | |
| | 1.0 | 458 | 4900 | | |
| **3** | 0.4 | 445 | 4850 | 430 | 3590 |
| | 0.6 | 445 | 4400 | | |
| | 0.8 | 446 | 4850 | | |
| | 1.0 | 447 | 4800 | | |
| **4** | 0.4 | 432 | 5500 | 415 | 4470 |
| | 0.6 | 432 | 5850 | | |
| | 0.8 | 431 | 6500 | | |
| | 1.0 | 430 | 5950 | | |
| **5** | 0.4 | 404 | 3450 | 395 | 4510 |
| **6** | 0.4 | 435 | 4050 | 424 | 3930 |
| | 0.6 | 438 | 4350 | | |
| | 0.8 | 440 | 4300 | | |
| | 1.0 | 440 | 4100 | | |
| **7** | 0.4 | 422 | – | 413 | 5250 |
| | 0.6 | 420 | 5200 | | |
| | 0.8 | 418 | – | | |
| | 1.0 | 420 | 5300 | | |
| **8** | 0.4 | 459 | 4000 | 443 | 3500 |
| | 0.6 | 461 | 4650 | | |
| **9** | 0.4 | 443 | 3850 | 428 | 3670 |
| | 0.6 | 445 | 4700 | | |
| | 0.8 | 447 | 4250 | | |
| | 1.0 | 448 | 4100 | | |
| **10** | 0.4 | 440 | 5150 | 418 | 4380 |
| | 0.6 | 442 | 5000 | | |
| | 0.8 | 435 | 5800 | | |
| **11** | 0.4 | 391 | – | 393 | 4400 |
| **12** | 0.4 | 442 | 3850 | 425 | 3730 |
| | 0.6 | 442 | 4350 | | |
| | 1.0 | 446 | 4850 | | |

Downloaded by [University of California, San Diego] at 12:25 07 August 2012

Downloaded by [University of California, San Diego] at 12:25 07 August 2012

recorded. Fizgure 7 displays the exemplary long-wavelength absorption spectra of the Langmuir film formed of dye **3**. The spectra were recorded before compression process (curve 1) and next at various surface pressures (curves 2-5). It is seen that there is no significant change in the shape and the peak position with the variation of the surface pressure and the increase of the absorbance with rising $\pi$ value is observed. However, the absorption of the Langmuir films was very small, even at high $\pi$, and the spectra were strongly noised. Therefore, it was difficult to visualize the maximum position, but upon appropriate processing the spectra (multiple smoothing of the curve by using OriginLab program), the maximum positions ($\lambda_{max}$) ) were identified and they are given in Table 2, together with the half-bandwidth ($\delta$) values. For comparison, the position of the absorption maximum and half-bandwidth of the long-wavelength absorption band of dyes **1**–**12** dissolved in chloroform at $X_M = 10^{-7}$ are also given in this Table. Figure 8 shows normalized long-wavelength absorption spectra of dye **9** in the Langmuir film at $\pi = 10.5$ mN/m and dissolved in chloroform at $X_M = 10^{-7}$. The spectra in chloroform are characteristic for monomeric absorption of naphthalimide dyes. The maximum position of the absorption band in the Langmuir film for all the dyes is shifted to the longer wavelength with respect to that in the diluted solution. Moreover, in monolayers spread on the water, the broadening of the absorption band of dyes **1**–**12** and their mixtures with 7CB is seen. These observations could suggest that in the monolayers at the air–water interface some fraction of self-aggregates by dye molecules is created, similarly as it was assumed in the case of Langmuir-Blodgett films of 1,8-naphthalimide dyes [5,6].

If sufficiently strong electronic transitions exist in molecules, the exciton splitting of excited states in molecular aggregates can be observed [19,20]. Large molar extinction coefficient of over 10 000 $dm^3 \cdot mol^{-1} \cdot cm^{-1}$ calculated for dyes **1**–**12** [2] indicate that the exciton coupling in the Langmuir films can be expected. Assuming the parallel configuration of naphthalimide dyes molecules in the simplest aggregate consisted of two molecules (dimer), the co-planar arrangement of the absorption transition moments can be considered. Then, according to the exciton molecular

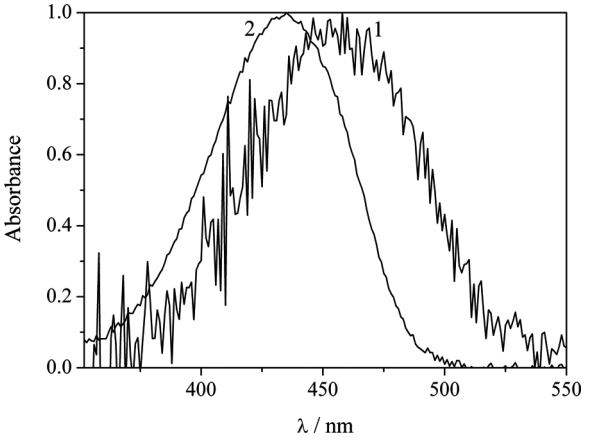


**Figure 8.** Normalized long-wavelength absorption spectrum *in situ* of the Langmuir film formed of dye **9** at $\pi = 10.5$ mN/m (1) and normalized long-wavelength absorption spectrum of dye **9** dissolved in chloroform at $X_M = 10^{-7}$ (2).

model proposed by Kasha *et al.* [16], the absorption band of dimer can be shifted towards shorter (blue) or longer (red) wavelengths with respect to that of monomer. The blue shift is indicative to creation of so-called H-type aggregates, i.e., dimers or higher order aggregates in which the dipole transition moments of molecules are parallel to each other and ordered perpendicularly to the stacking direction. The red shift is characteristic for so-called J-type aggregates in which dipole transition moments are parallel to each other but greatly inclined from the normal to the stacking direction [17].

The broadening of the absorption band with the red shift of the maximum position in the case of derivatives of 4-aminonaphthalimide can be due to the formation of some fraction of J-type aggregates among dye **1**–**12** molecules in the Langmuir films.

Downloaded by [University of California, San Diego] at 12:25 07 August 2012

## 4. Conclusions

The creation of the stable Langmuir films from derivatives of 4-aminonaphthalimide depends strongly on the molecular structure of both substituents to the main core of the molecule. Except of dyes **5** and **11**, having morpholine ring in the substituent R, all other dyes under investigation are able to create themselves stable and compressible monolayers at the water surface. The detailed analysis of the shapes of the $\pi$-A and $\Delta$V-A isotherms for the Langmuir films formed from binary mixtures of dyes **1**–**12** with 7CB allows to ascertain that the packing density of molecules as well as the rigidity and the stability of the monolayer at the air–water interface depend strongly not only on the molecular structure of both components but also on the film composition. This observation is confirmed by the film textures obtained by means of Brewster angle microscope. From the electronic absorption spectra recorded *in situ* follows that the high concentration of the dye in the Langmuir film generates favorable conditions for the creation of self-aggregates by molecules of 1,8-naphthalimide dyes, already in the ground electronic state.

## Acknowledgment

This work was supported by Research Project No. N N202 238037, coordinated by Ministry of Science and Higher Education.

## References

[1] Martyński, T., Mykowska, E., & Bauman, D. (1994). *J. Mol. Structure*, *325*, 161.
[2] Bielejewska, N., Wolarz, E., Stolarski, R., & Bauman, D. (2008). *Opto-Electron. Rev.*, *16*, 367.
[3] Żmija, J., Zieliński, J., Parka, J., & Nowinowski-Kruszelnicki, E. (1993). *Displeje ciekłokrystaliczne* (in Polish), PWN: Warszawa.
[4] Biadasz, A., Martyński, T., Stolarski, R., & Bauman, D. (2006). *Liq. Cryst.*, *33*, 307.
[5] Bielejewska, N., Stolarski, R., & Bauman, D. (2009). *Z. Naturforsch.*, *64a*, 492.
[6] Bielejewska, N., Chrzumnicka, E., Stolarski, R., & Bauman, D. (2010) Opto-Electron. Rev., *18*, 197.
[7] Biadasz, A., Łabuszewska, K., Chrzumnicka, E., Michałowski, E., Martyński, T., & Bauman, D. (2007) *Dyes Pigments*, *74*, 598.
[8] Petty, M. C. (1996). *Langmuir-Blodgett Films-An Introduction*, Cambridge University Press: Cambridge.

[9] Stolarski, R. (2009). *Fibres and Textiles in Eastern Europe*, *17*, 91.
[10] Hoenig, D., & Moebius, D. (1991). *J. Phys. Chem.*, *95*, 4590.
[11] Gaines, G. L. (1996). *Insoluble Monolayers at Liquid-Gas Interface*, New York: Interscience.
[12] Inglot, K., Martyński, T., & Bauman, D. (2009). *Dyes and Pigments*, *80*, 106.
[13] Inglot, K., Martyński, T., & Bauman, D. (2006). *Liq. Cryst.*, *33*, 855.
[14] Friedenberg, M. C., Fuller, G. C., Frank, C., & Robertson, C. R. (1994). *Langmuir 10*, 1251.
[15] Myers, D. (1999). *Surfaces, Interfaces and Colloids*, Willey-VCH: New York.
[16] Kasha, M., Rawls, H. R., & Ashraf El-Bayoumi, M. (1965). *Pure Appl.Chem. 11*, 371.
[17] Moebius, D. (1995). *Adv.Mater. 5*, 437.

Downloaded by [University of California, San Diego] at 12:25 07 August 2012